NACA RM L54A19

NACA

RESEARCH MEMORANDUM

EXPERIMENTAL AND CALCULATED STATIC CHARACTERISTICS OF A TWO-BLADE NACA 10-(3)(062)-045 PROPELLER

By John M. Swihart

Langley Aeronautical Laboratory
Langley Field, Va.

NATIONAL ADVISORY COMMITTEE
FOR AERONAUTICS

WASHINGTON
March 12, 1954

NATIONAL ADVISORY COMMITTEE FOR AERONAUTICS

RESEARCH MEMORANDUM

EXPERIMENTAL AND CALCULATED STATIC CHARACTERISTICS OF A TWO-BLADE NACA 10-(3)(062)-045 PROPELLER

By John M. Swihart

SUMMARY

An investigation has been conducted to determine the static characteristics of a two-blade NACA 10-(3)(062)-045 propeller. Experimental data were obtained for a blade-angle range from -5° to 40° measured at the 0.75 radial station and for tip Mach numbers up to 1.0. Comparisons of experimental data with thrust and power coefficients calculated by strip theory show good agreement where adequate airfoil data are available. At any given blade angle the static thrust figure of merit increases with increasing tip Mach number for values of tip Mach number up to 1.0. Mild stall flutter occurred at the higher blade angles limiting the rotational speed to tip Mach numbers less than 1.0.

INTRODUCTION

The results of static thrust tests of propellers varying in camber (for example, ref. 1) have shown that the static thrust characteristics vary widely depending on the type of airfoil sections used in the propeller design. Therefore, methods for estimating static thrust, which are based on tests of propellers incorporating Clark Y or RAF 6 airfoil sections (for example, refs. 2 to 4), may yield erroneous results when used to estimate the static thrust of propellers with NACA 16-series or other low-drag airfoil sections. Although some data have been published on propellers of low-drag airfoil sections, the lack of a complete range of such data makes it desirable to check the applicability of strip theory for the calculation of static thrust and power characteristics as a method of surmounting the inadequacies of references 2 to 4.

A strip-theory method for determining the static characteristics of a propeller is presented in this paper. The treatment accounts for a finite number of blades by use of the Lock-Goldstein factor and for compressibility effects by use of airfoil data obtained at high speeds.

The purpose of the present paper is to augment the experimental data on propellers incorporating NACA 16-series airfoil sections with the results from an investigation on the Langley propeller static test stand of a two-blade NACA 10-(3)(062)-045 propeller. Additional purposes were to provide data for comparison with an empirical method for estimating propeller static characteristics (ref. 2) and for comparison with the more tedious strip-theory analysis. The tests covered a range of blade angles from -5° to 40° measured at the 0.75 radial station and tip Mach numbers up to 1.0.

SYMBOLS

B	number of blades
b	blade width
c_d	section drag coefficient
c_l	section lift coefficient
c_{l_d}	design blade section lift coefficient
C_P	power coefficient, $\frac{P}{\rho n^3 D^5}$
C_T	thrust coefficient, $\frac{T}{\rho n^2 D^4}$
C_T/C_P	static thrust figure of merit
D	propeller diameter
ΔD	drag of a blade element
G	Lock-Goldstein induced-velocity-correction factor for a finite number of blades
h	blade thickness
ΔL	lift of a blade element
M_t	tip Mach number, based on rotational speed of propeller tip

M_x	Mach number of station x, $M_t x \cos \phi$
N	propeller rotational speed, rpm
n	propeller rotational speed, rps
P	power
Q	torque
$\Delta Q/r$	force resisting propeller rotation
R	propeller-tip radius
ΔR	resultant force on a blade element
r	radius to station x
T	thrust
V	axial velocity
W	resultant velocity at blade section, $\pi n D x \cos \phi$
w_i	induced velocity at blade section
x	fraction of propeller-tip radius, r/R
β_x	blade angle at station x, deg
$\gamma = \tan^{-1} \frac{c_d}{c_l}$	
ρ	air density
σ	total propeller solidity, $Bb/\pi Dx$
ϕ	aerodynamic helix angle, $\tan^{-1} \frac{w_i}{W}$, deg

Subscripts:

0, 1, 2, 3, etc. order of approximation

APPARATUS

6,000-Horsepower Propeller Dynamometer

The dynamometer power was supplied by two 3,000-horsepower induction motors mounted on vertical support struts of circular-arc airfoil section. The two units can be operated independently of one another or coupled and operated as a single 6,000-horsepower unit. Figure 1 shows the dynamometer at the Langley propeller static test stand as it was used for this investigation. Reference 1 gives a detailed description of the dynamometer and its principal arrangements.

Propeller

The propeller used for this investigation was constructed of solid Duralumin and was designated a two-blade NACA 10-(3)(062)-045 propeller. The numerals in the propeller designation give: the diameter in feet, 10; and the following design conditions at the 0.7 radial station: design lift coefficient, 0.3; thickness ratio, 0.062; and solidity per blade, 0.045. Figure 2 shows the propeller mounted on the dynamometer. The propeller blade-form curves are shown in figure 3. The spinner surface is located at $x = 0.267$. A 32-inch-diameter spinner and spinner-cover plates were used in this investigation (see fig. 2).

TESTS, DATA REDUCTION, AND ACCURACY

Tests

Thrust, torque, and rotational speed were measured at intervals of 100 rpm from 600 rpm to 2,200 rpm or until stall flutter occurred. At the highest blade angle, data were taken starting at 450 rpm. These propeller blades had not been whirl tested above 2,200 rpm because this was considered a marginally safe speed; therefore the maximum rotational speed was limited to 2,200 rpm during these aerodynamic tests.

Data Reduction

The thrust and power data have been reduced to the nondimensional coefficients C_T and C_P.

The calculated coefficients are based on the forces acting on a blade element (see fig. 4) and the equations for section thrust and power

coefficients are derived for the static case when $V = 0$ using propeller vortex theory with the Lock-Goldstein correction for finite number of blades.

The equations derived for section thrust and power coefficients in this paper are:

$$\frac{dC_T}{dx} = \frac{B}{4}(\pi x)^2 \cos^2\phi \frac{\cos(\phi + \gamma)}{\cos \gamma} \frac{b}{D} c_l$$

$$\frac{dC_P}{dx} = \frac{B}{4}(\pi x)^3 \cos^2\phi \frac{\sin(\phi + \gamma)}{\cos \gamma} \frac{b}{D} c_l$$

The values of C_T and C_P are found by integration of the grading curves. The derivation and the method of calculation are given in the appendix.

Accuracy of Experimental Data

The wind velocity at the test facility was measured by a sensitive hot-wire anemometer and for this investigation no test was made when the wind velocity was greater than 2.5 mph. No corrections to the data are believed to be necessary for wind velocities of this magnitude.

The static calibration of the thrust and torque measuring systems indicates a probable error of ±3.5 pounds of thrust and ±2.9 foot-pounds of torque (see ref. 1). Duplicate tests at the same conditions show C_T and C_P to be repeated within ±0.003. The rotational speed of the dynamometer can be set to ±1/4 rpm.

RESULTS AND DISCUSSION

A comparison of the experimental data with the calculated results from the strip-theory analysis and with results obtained from the working charts of reference 2 is presented in figure 5. The strip theory is shown to be in good agreement with the experimental data at the low blade angles (4° and 10°) and in fair agreement at a blade angle of 15°. The lack of airfoil data for the correct camber and thickness ratio at high angles of attack and high subsonic Mach numbers prevented reliable calculation for blade angles greater than 15°, and it was necessary to extrapolate some of the existing airfoil data to obtain section thrust and

power coefficients for the inboard stations at $\beta_{0.75R} = 15^\circ$. Because the power coefficients measured at blade angles of 4° and 10° were less than the smallest value of power coefficient for which thrust data are presented in reference 2, the thrust coefficient could not be obtained from the working charts of reference 2 for these blade angles. The power coefficients used to obtain the thrust coefficient from the working charts at 15° and 20° blade angles were the values measured for these blade angles. In spite of the limitations to the strip-theory analysis (the necessity for extrapolation of the airfoil data) at the 15° blade-angle setting, the agreement is much better than that shown for the method of reference 2. The working charts yield results which are very optimistic at a blade angle of 20°.

Variation of static characteristics with tip Mach number.- Figure 6 shows the variation of C_T and C_P with tip Mach number for all blade angles tested. The increased slope of the C_T and C_P curves with increasing tip Mach numbers would be expected because most of the blade sections are operating at subcritical speeds and develop higher lift-curve slopes in accordance with the Prandtl-Glauert relation (ref. 5). Stall flutter limited the rotational speed at blade angles of 20°, 30°, and 40°. Because the blade torsional oscillations were not measured during these tests, stall flutter was detected audibly and was sometimes difficult to distinguish from the ordinary propeller noise at these high blade angles.

Variation of static characteristics with blade angle at a constant tip Mach number.- The variation of the thrust coefficient, the power coefficient, and the static thrust figure of merit with blade angle at a tip Mach number of 0.3 are shown in figure 7. The propeller coefficient curves are analogous to the variation of lift and drag coefficients and lift-to-drag ratio with angle of attack for a wing. One difference is apparent in that the thrust-coefficient curve does not show a marked stall at the high blade angles. This difference is probably due to the pitch distribution (different blade sections stalling at different times).

Effect of tip speed.- The static thrust figure-of-merit variation with power coefficient is presented in figure 8 for tip Mach numbers of 0.3, 0.7, and 1.0. The maximum value of C_T/C_P is obtained at a tip Mach number of 1.0 and there is an increase in C_T/C_P for all power coefficients at $M_t = 1.0$ when compared with the lower tip Mach numbers. The results of reference 5 indicate an increase in section lift-drag ratio with an increase in Mach number below the critical speed. Since most of the blade sections are operating at subcritical speeds when the rotational tip Mach number is 1.0, an increase in C_T/C_P would be expected. Stall flutter limited the rotational speed at the higher blade angles and power coefficients greater than about 0.086 could not be obtained at a tip Mach number of 1.0 because of the flutter limitation.

CONCLUDING REMARKS

An investigation has been conducted to determine the static characteristics of a two-blade NACA 10-(3)(062)-045 propeller and to compare the experimental data with results calculated by strip theory. The strip-theory analysis can be used to predict the static propeller characteristics if airfoil data are available for the correct Mach number, angle of attack, camber, and thickness ratio. The strip theory yields better results than an empirical method.

At any given blade angle the static thrust figure of merit increases with increasing tip Mach number for values of tip Mach number up to 1.0.

Langley Aeronautical Laboratory,
National Advisory Committee for Aeronautics,
Langley Field, Va., January 6, 1954.

APPENDIX

For a propeller operating under static conditions the helix angle ϕ is the induced angle. From reference 6, the induced velocity w_i normal to the helical vortex sheet for a propeller having a finite number of blades is

$$w_i = \frac{\sigma c_l W}{4G \sin \phi}$$

From the section velocity vector diagram (fig. 4)

$$\tan \phi = \frac{w_i}{W} = \frac{\sigma c_l}{4G \sin \phi}$$

or

$$\sigma c_l = 4G \sin \phi \tan \phi$$

Values of the Lock-Goldstein factor are given in reference 7 as a function of $\sin \phi$ and r/R for propellers having two, three, four, five, and six blades.

The lift force acting on a blade element is

$$\Delta L = \rho n^2 D^4 \frac{B}{4} (\pi x)^2 \cos^2 \phi c_l \frac{b}{D} \Delta x$$

The resultant of lift and drag forces acting on the blade element is

$$\Delta R = \frac{\Delta L}{\cos \gamma}$$

where

$$\gamma = \tan^{-1} \frac{\Delta D}{\Delta L}$$

From the resolution of forces on a blade element (fig. 4)

$$\Delta T = \Delta R \cos(\phi + \gamma)$$

$$\frac{\Delta Q}{r} = \Delta R \sin(\phi + \gamma)$$

Substitution of the expressions for ΔR and ΔL into the foregoing expressions for elemental thrust and torque force, and reduction to coefficient form, yields the radial gradients of thrust and power coefficient as

$$\frac{dC_T}{dx} = \frac{B}{4}(\pi x)^2 \frac{\cos^2\phi \cos(\phi + \gamma)}{\cos \gamma} \frac{b}{D} c_l$$

$$\frac{dC_P}{dx} = \frac{B}{4}(\pi x)^3 \frac{\cos^2\phi \sin(\phi + \gamma)}{\cos \gamma} \frac{b}{D} c_l$$

The procedure used to evaluate these equations was as follows:

(1) Select a value of ϕ_0 to be about one-half the blade angle at station x, β_x. Then $\alpha_0 = \beta_x - \phi_0$ and $M_{x_0} = M_t x \cos \phi_0$.

(2) For these values of α_0 and M_{x_0} select the corresponding value of c_{l_0} from airfoil data (obtained from refs. 5 and 8).

(3) Multiply c_{l_0} by b/D at station x and select the proper value of ϕ_1 from table I. Values of ϕ are presented in table I as a function of $\frac{b}{D} c_l$ and x for two-, three-, and four-blade propellers. These values represent a solution of the equation $\sigma c_l = 4G \sin \phi \tan \phi$ for the static case, for which the data were obtained from references 6 and 7. Because ϕ_1 does not equal ϕ_0, the procedure is repeated using ϕ_1. Sometimes a fourth approximation is necessary to stabilize α, that is, before $\phi_3 = \phi_4$. When c_l and ϕ have been determined for each blade station, the thrust and power gradients can be calculated. Integration of these thrust and power grading curves will give the propeller thrust and power coefficients for the selected operating condition.

REFERENCES

1. Wood, John H., and Swihart, John M.: The Effect of Blade-Section Camber on the Static Characteristics of Three NACA Propellers. NACA RM L51L28, 1952.

2. Desmond, Gerald L., and Freitag, Robert F.: Working Charts for the Computation of Propeller Thrust Throughout the Take-off Range. NACA WR W-100, 1943. (Formerly NACA ARR No. 3G26.)

3. Diehl, Walter S.: Static Thrust of Airplane Propellers. NACA Rep. 447, 1932.

4. Haines, A. B., and Chater, P. B.: Revised Charts for the Determination of the Static and Take-Off Thrusts of a Propeller. R. & M. No. 2358, British A.R.C., 1950.

5. Lindsey, W. F., Stevenson, D. B., and Daley, Bernard N.: Aerodynamic Characteristics of 24 NACA 16-Series Airfoils at Mach Numbers Between 0.3 and 0.8. NACA TN 1546, 1948.

6. Lock, C. N. H., and Yeatman, D.: Tables for Use in an Improved Method of Airscrew Strip Theory Calculation. R. & M. No. 1674, British A.R.C., 1935.

7. Lock, C. N. H., Pankhurst, R. C., and Conn, J. F. C.: Strip Theory Method of Calculation for Airscrews on High-Speed Aeroplanes. R. & M. No. 2035, British A.R.C., 1945.

8. Anon.: Propeller Performance Analysis. Aerodynamic Characteristics, NACA 16 Series Airfoils. Rep. No. C-2000, Pt. II, Curtiss-Wright Corp., Propeller Div. (Caldwell, N. J.), Dec. 2, 1948.

TABLE I.- INDUCED ANGLE ϕ AS A FUNCTION OF BLADE GEOMETRY FOR STATIC CONDITIONS

ϕ, deg	Values of $\frac{b}{D} c_l$ for -								
	x = 0.30	x = 0.45	x = 0.60	x = 0.70	x = 0.75	x = 0.80	x = 0.85	x = 0.90	x = 0.95
					B = 2				
1	0.0006	0.0009	0.0011	0.0013	0.0014	0.0015	0.0016	0.0017	0.0018
2	.0023	.0034	.0046	.0054	.0057	.0061	.0065	.0068	.0065
3	.0052	.0078	.0103	.0121	.0129	.0137	.0144	.0146	.0127
4	.0092	.0138	.0184	.0214	.0228	.0239	.0247	.0239	.0200
5	.0144	.0215	.0287	.0333	.0352	.0366	.0370	.0349	.0285
6	.0207	.0310	.0413	.0477	.0501	.0514	.0509	.0474	.0377
7	.0282	.0422	.0559	.0641	.0670	.0681	.0667	.0613	.0482
8	.0368	.0551	.0729	.0827	.0858	.0863	.0836	.0762	.0592
9	.0466	.0697	.0918	.1031	.1065	.1063	.1019	.0919	.0708
10	.0575	.0860	.1125	.1250	.1281	.1268	.1205	.1077	.0822
11	.0696	.1040	.1352	.1486	.1512	.1488	.1402	.1246	.0943
12	.0827	.1234	.1589	.1730	.1747	.1713	.1605	.1414	.1063
13	.0970	.1446	.1842	.1985	.1992	.1942	.1811	.1589	.1184
14	.1123	.1671	.2106	.2247	.2243	.2177	.2020	.1764	.1307
15	.1289	.1908	.2384	.2517	.2500	.2412	.2226	.1937	.1432
16	.1465	.2163	.2673	.2795	.2764	.2654	.2444	.2110	.1552
17	.1651	.2431	.2976	.3082	.3033	.2902	.2668	.2295	.1681
18	.1849	.2708	.3282	.3370	.3303	.3150	.2885	.2464	.1798
19	.2058	.3001	.3596	.3668	.3582	.3398	.3107	.2637	.1927
20	.2276	.3305	.3928	.3970	.3866	.3655	.3338	.2816	.2058
					B = 3				
1	0.0004	0.0006	0.0008	0.0009	0.0010	0.0010	0.0011	0.0011	0.0012
2	.0015	.0023	.0031	.0036	.0038	.0041	.0043	.0045	.0045
3	.0034	.0052	.0069	.0080	.0086	.0092	.0097	.0100	.0094
4	.0061	.0092	.0123	.0143	.0153	.0162	.0170	.0171	.0152
5	.0096	.0144	.0191	.0223	.0239	.0252	.0261	.0258	.0222
6	.0138	.0207	.0276	.0322	.0344	.0359	.0369	.0357	.0297
7	.0188	.0281	.0375	.0436	.0463	.0482	.0489	.0468	.0382
8	.0245	.0368	.0491	.0567	.0600	.0620	.0622	.0588	.0472
9	.0311	.0466	.0620	.0715	.0744	.0771	.0768	.0717	.0569
10	.0384	.0575	.0764	.0877	.0920	.0935	.0921	.0850	.0668
11	.0465	.0697	.0923	.1055	.1099	.1111	.1086	.0990	.0773
12	.0553	.0829	.1096	.1243	.1288	.1297	.1255	.1136	.0883
13	.0649	.0973	.1282	.1442	.1491	.1493	.1437	.1288	.0998
14	.0754	.1129	.1481	.1654	.1703	.1696	.1621	.1444	.1114
15	.0866	.1297	.1692	.1877	.1922	.1906	.1810	.1603	.1231
16	.0986	.1475	.1915	.2109	.2153	.2121	.2001	.1767	.1349
17	.1115	.1664	.2153	.2354	.2390	.2348	.2205	.1938	.1469
18	.1250	.1865	.2400	.2603	.2634	.2575	.2406	.2105	.1595
19	.1395	.2075	.2655	.2860	.2881	.2803	.2614	.2274	.1717
20	.1547	.2296	.2922	.3132	.3141	.3041	.2828	.2455	.1842
					B = 4				
1	0.0003	0.0004	0.0006	0.0006	0.0007	0.0008	0.0008	0.0009	0.0009
2	.0011	.0017	.0023	.0027	.0029	.0031	.0033	.0034	.0036
3	.0026	.0039	.0050	.0060	.0065	.0069	.0073	.0077	.0077
4	.0046	.0069	.0092	.0107	.0115	.0122	.0130	.0135	.0126
5	.0072	.0108	.0144	.0168	.0180	.0191	.0202	.0208	.0184
6	.0104	.0155	.0207	.0241	.0259	.0274	.0288	.0290	.0249
7	.0141	.0212	.0282	.0328	.0351	.0371	.0387	.0382	.0324
8	.0184	.0276	.0368	.0429	.0458	.0482	.0499	.0484	.0402
9	.0233	.0350	.0466	.0543	.0579	.0605	.0619	.0592	.0487
10	.0288	.0432	.0575	.0670	.0711	.0739	.0747	.0705	.0575
11	.0349	.0523	.0696	.0809	.0855	.0883	.0883	.0828	.0668
12	.0416	.0624	.0829	.0959	.1009	.1036	.1029	.0957	.0765
13	.0488	.0732	.0973	.1121	.1175	.1201	.1184	.1089	.0865
14	.0567	.0850	.1129	.1293	.1350	.1372	.1346	.1228	.0969
15	.0652	.0976	.1294	.1473	.1534	.1551	.1513	.1370	.1072
16	.0743	.1112	.1472	.1667	.1726	.1737	.1688	.1515	.1179
17	.0840	.1258	.1660	.1867	.1929	.1930	.1869	.1665	.1291
18	.0943	.1411	.1859	.2076	.2134	.2128	.2051	.1819	.1400
19	.1051	.1574	.2065	.2293	.2351	.2329	.2236	.1974	.1512
20	.1167	.1744	.2283	.2521	.2575	.2543	.2426	.2140	.1635

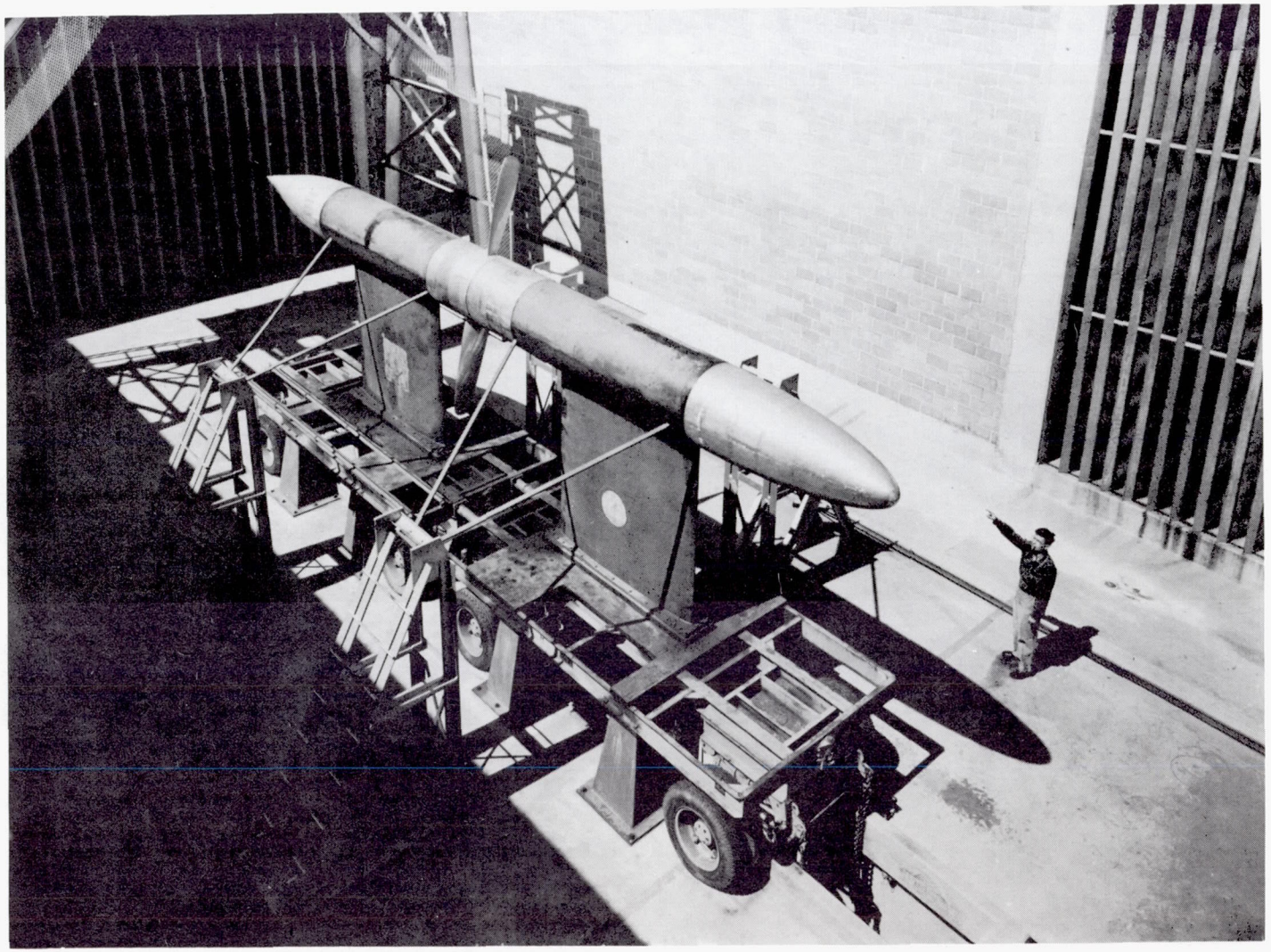

L-69807

Figure 1.- NACA 6000-horsepower propeller dynamometer at the Langley propeller static test stand.

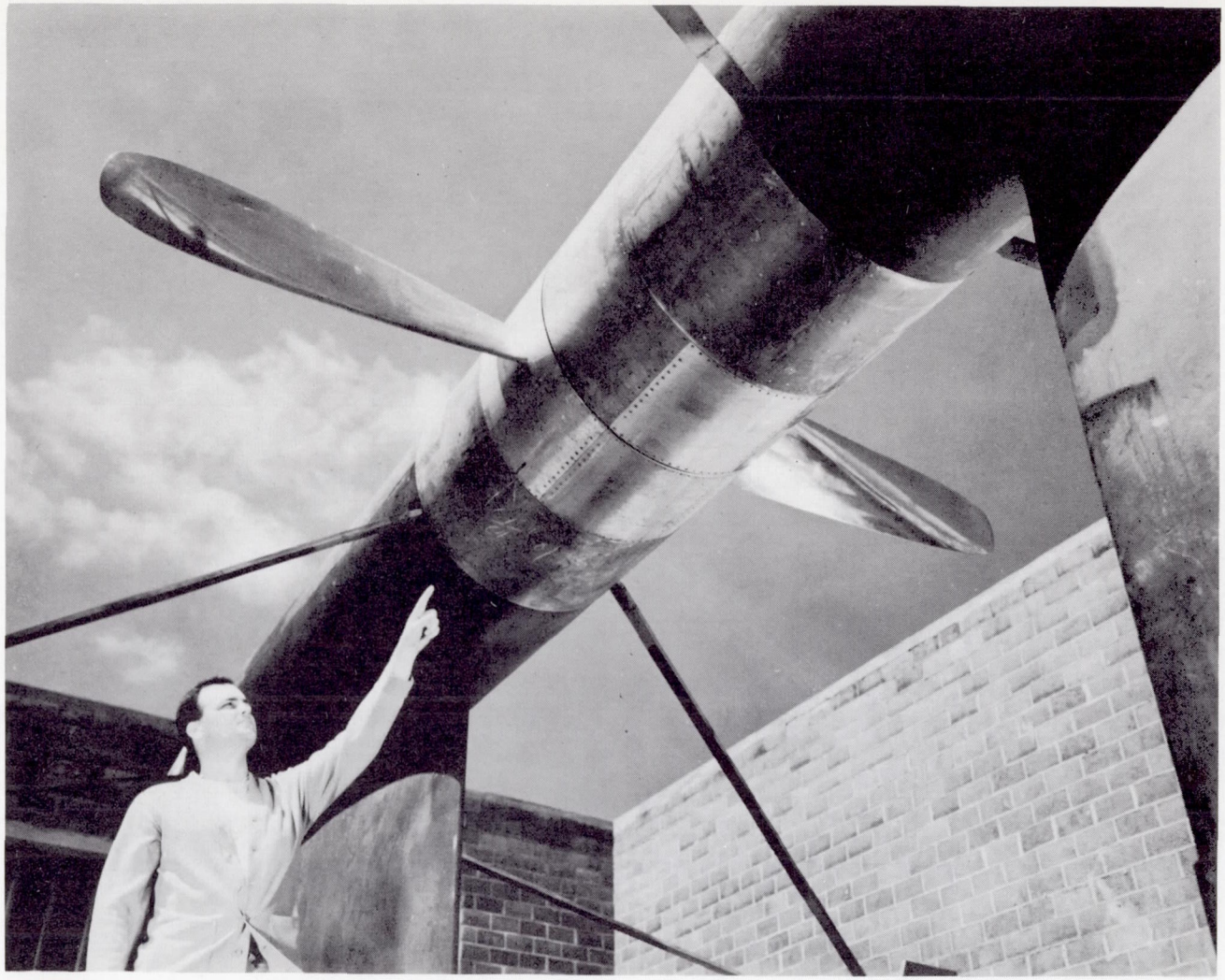

L-70311

Figure 2.- A two-blade NACA 10-(3)(062)-045 propeller mounted on the dynamometer.

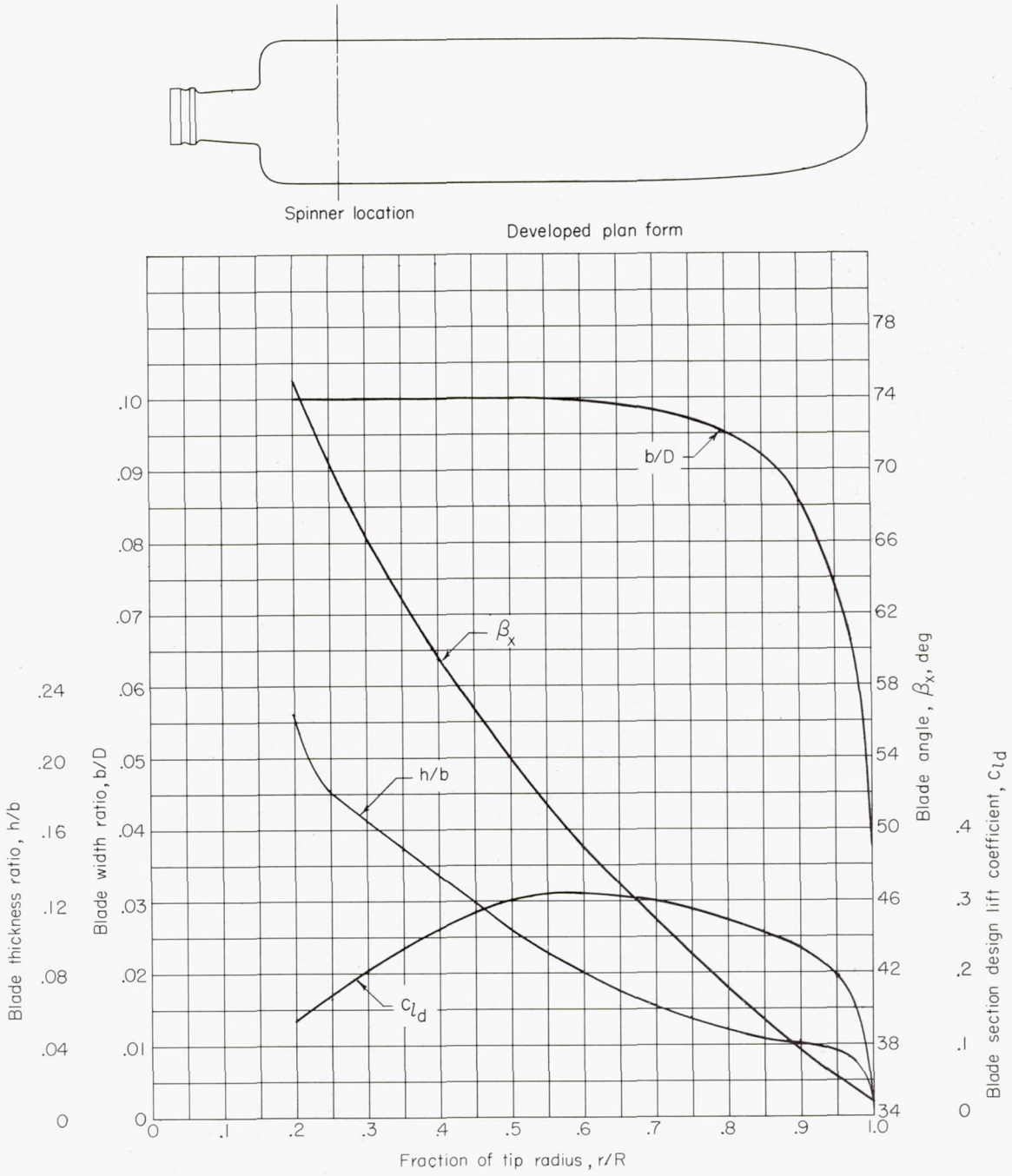

Figure 3.- Blade-form curves for NACA 10-(3)(062)-045 propeller.

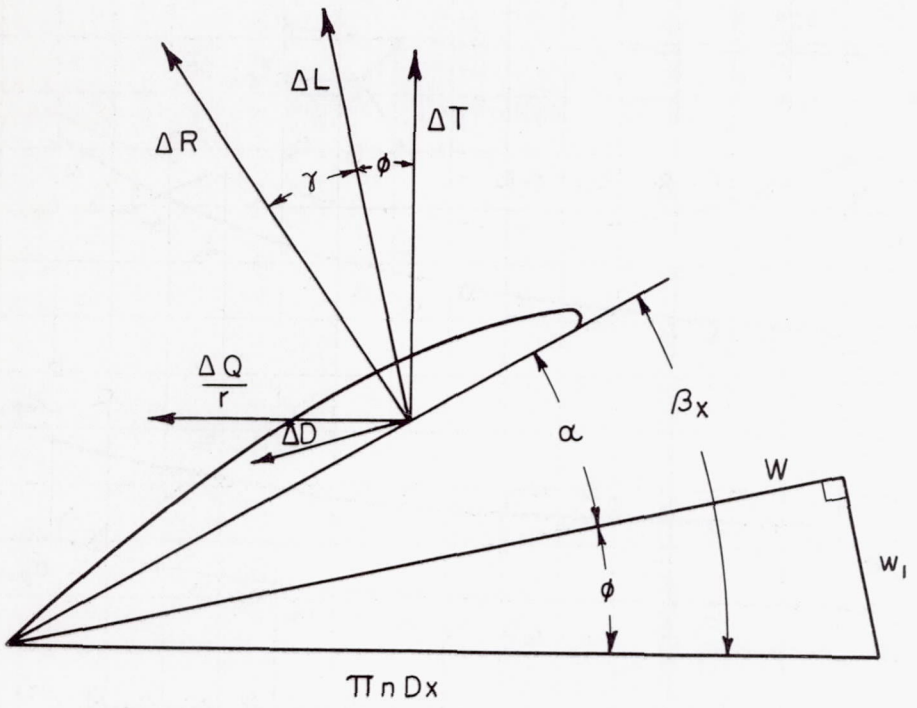

Figure 4.- Forces acting on a blade element.

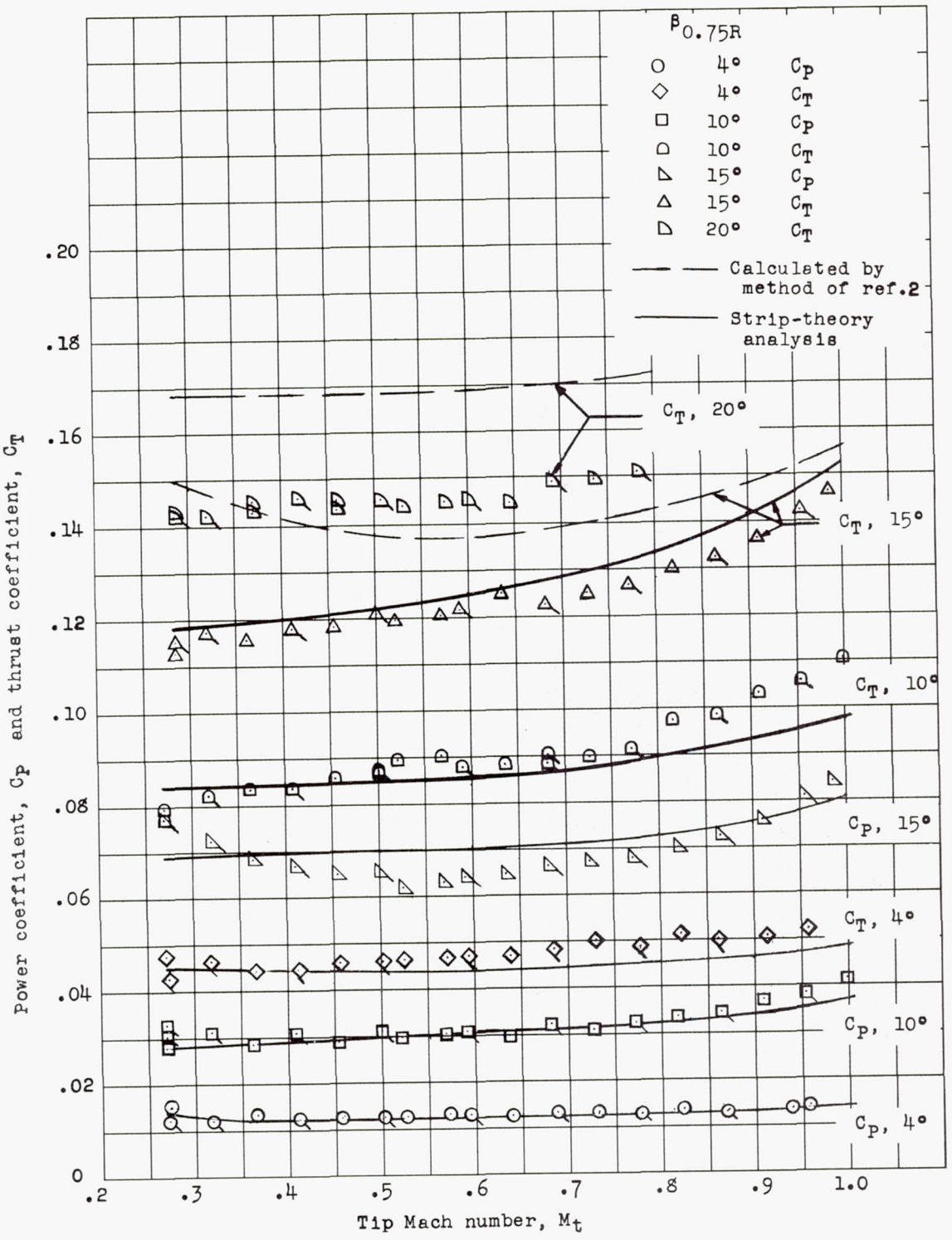

Figure 5.- Typical test results for the NACA 10-(3)(062)-045 two-blade propeller and a comparison with calculated values. Flagged symbols indicate data taken with the rpm decreasing.

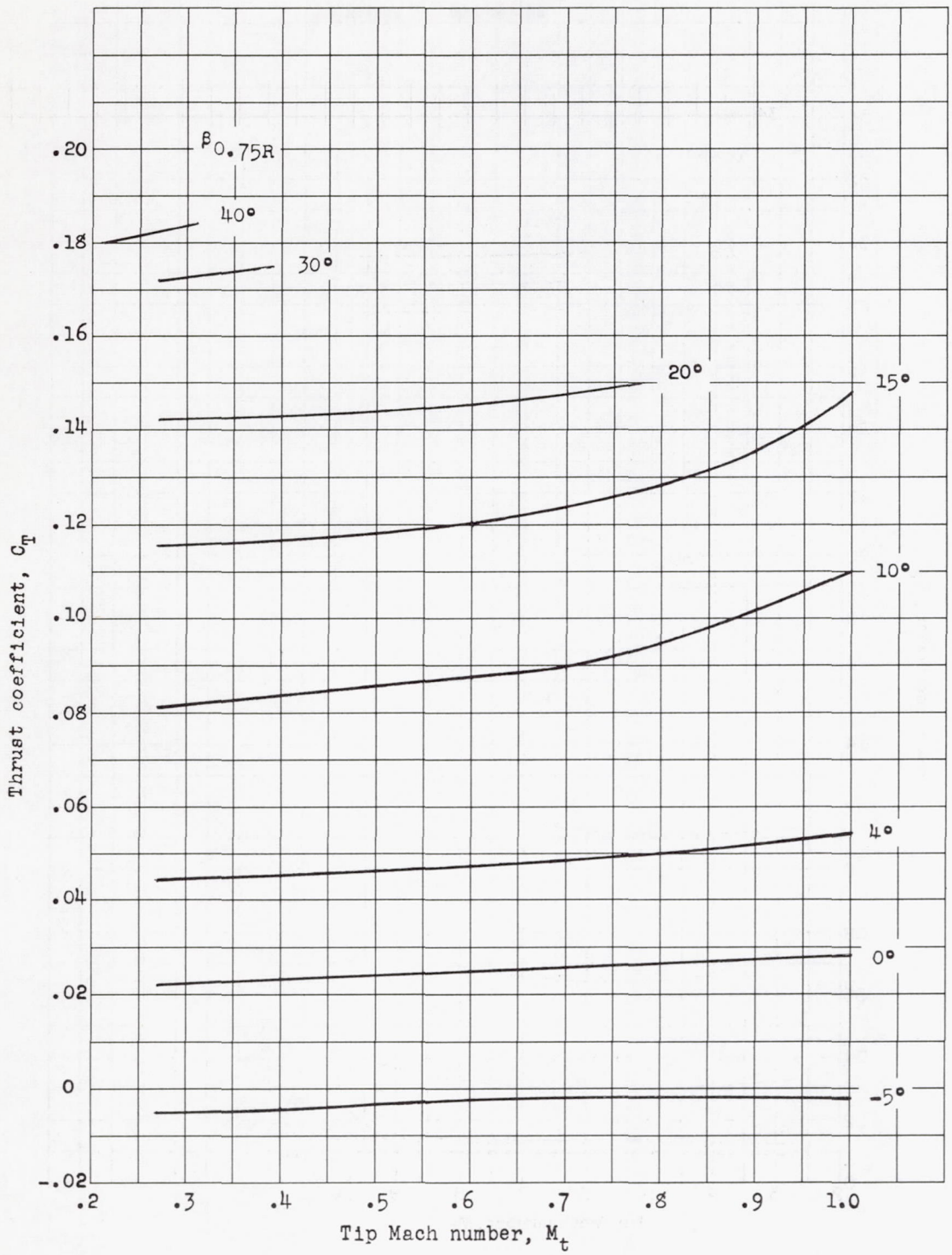

(a) Thrust coefficient.

Figure 6.- Variation of thrust and power coefficient with tip Mach number for a two-blade NACA 10-(3)(062)-045 propeller.

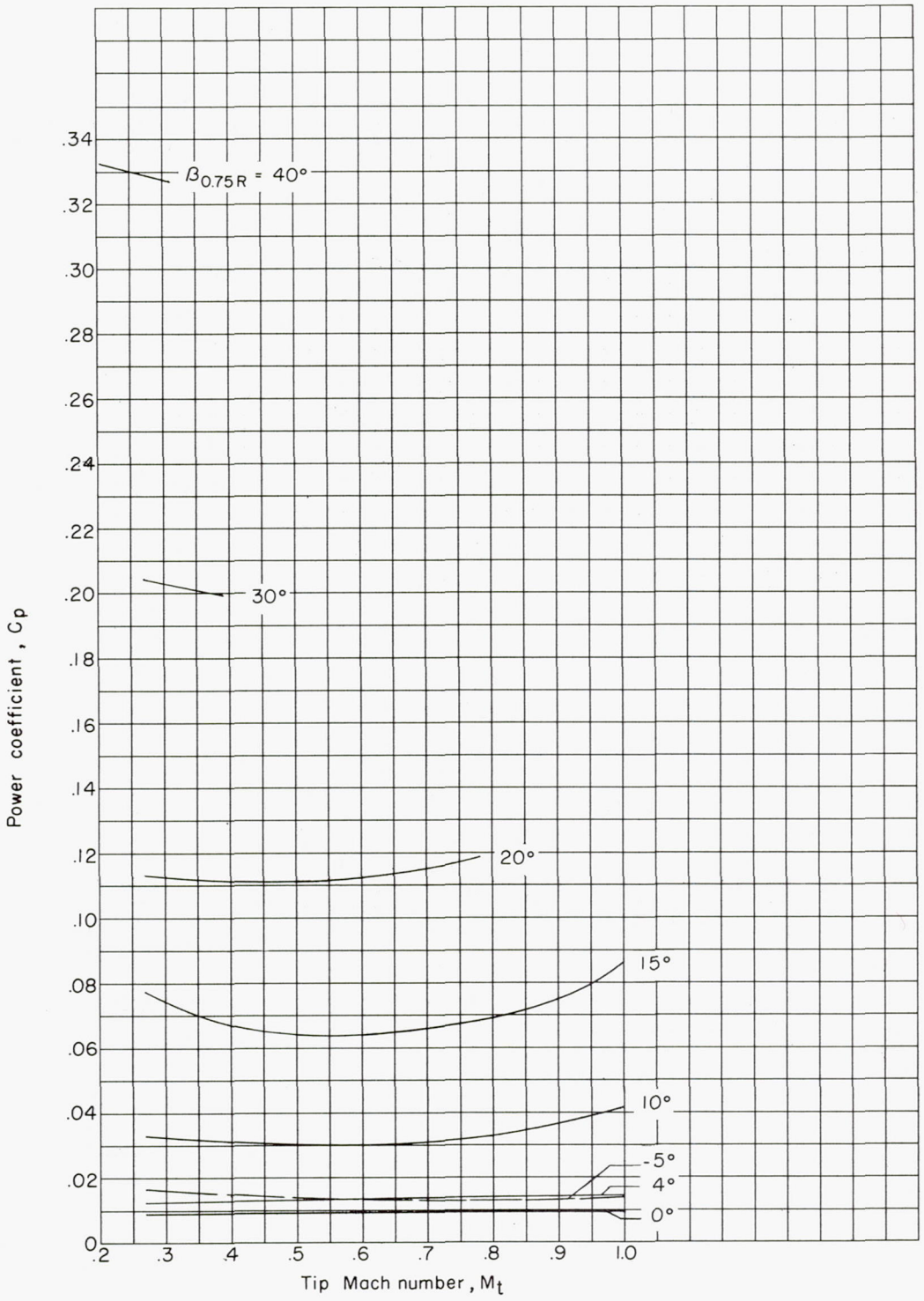

(b) Power coefficient.

Figure 6.- Concluded.

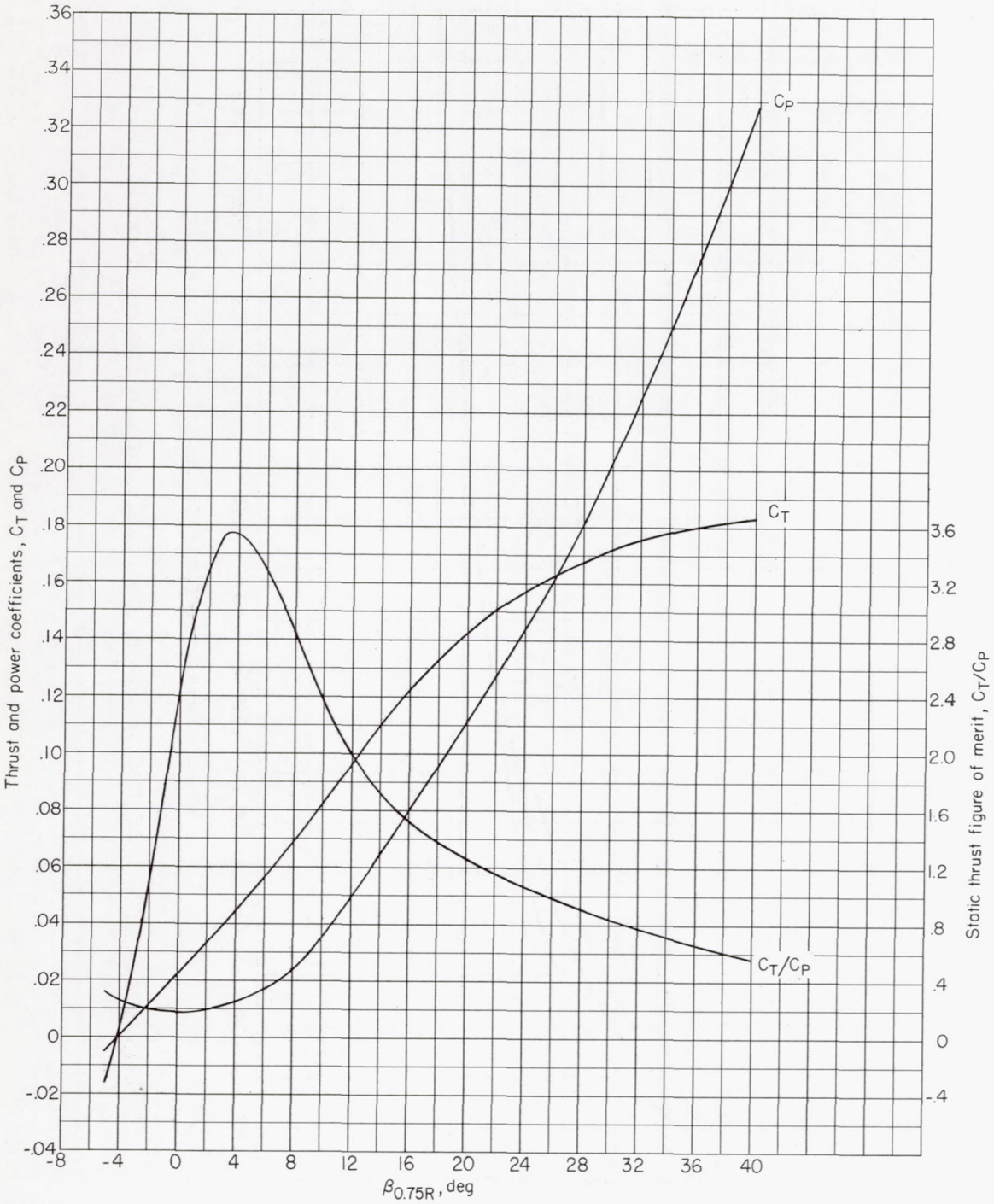

Figure 7.- Static characteristics of the two-blade NACA 10-(3)(062)-045 propeller at a tip Mach number of 0.3.

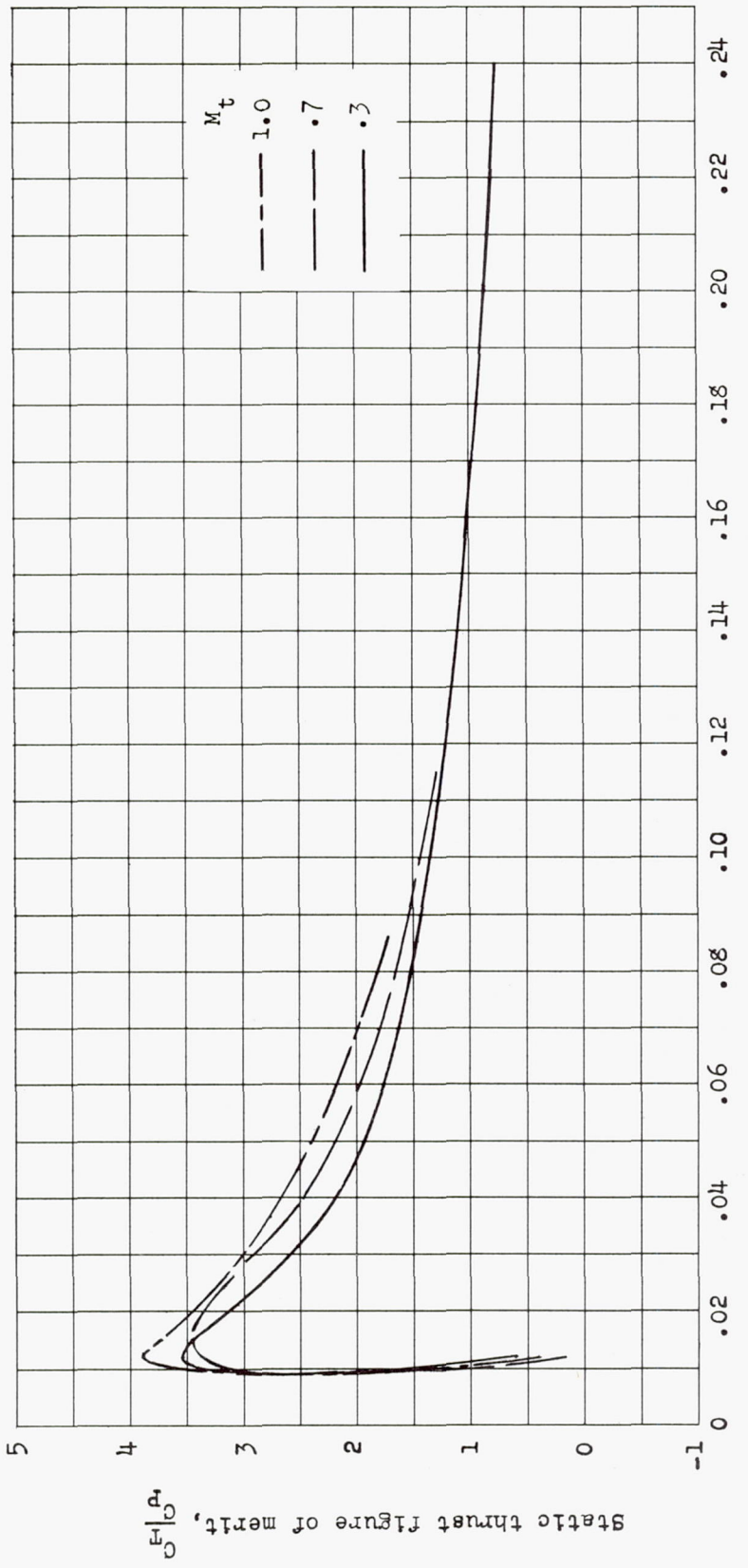

Figure 8.- Effect of tip speed on the static thrust figure of merit.

NACA-Langley - 3-12-54 - 325